Accepted Manuscript

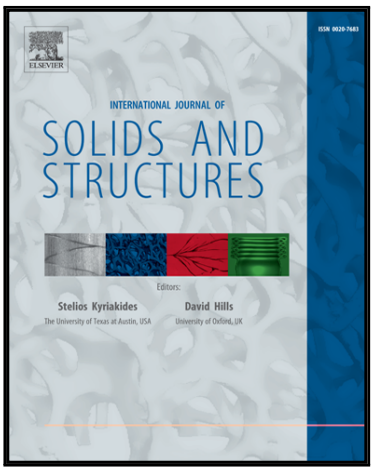

Optimization of Postbuckling Behaviour of Variable Thickness Composite Panels with Variable Angle Tows: Towards "Buckle-Free" Design Concept

Zhangming Wu, Gangadharan Raju, Paul M Weaver

PII: S0020-7683(17)30402-X
DOI: 10.1016/j.ijsolstr.2017.08.037
Reference: SAS 9716

To appear in: *International Journal of Solids and Structures*

Received date: 20 March 2017
Revised date: 21 August 2017
Accepted date: 31 August 2017

Please cite this article as: Zhangming Wu, Gangadharan Raju, Paul M Weaver, Optimization of Postbuckling Behaviour of Variable Thickness Composite Panels with Variable Angle Tows: Towards "Buckle-Free" Design Concept, *International Journal of Solids and Structures* (2017), doi: 10.1016/j.ijsolstr.2017.08.037

Optimization of Postbuckling Behaviour of Variable Thickness Composite Panels with Variable Angle Tows: Towards "Buckle-Free" Design Concept

Zhangming Wu[a,b], Gangadharan Raju[c], Paul M Weaver[d,e]

[a] *Cardiff School of Engineering, Queens Buildings, The Parade, Newport Road, Cardiff CF24 3AA, UK*
[b] *School of Aerospace Engineering and Applied Mechanics, Tongji University, 1239 Siping Road, Shanghai 200092, China*
[c] *Department of Mechanical and Aerospace Engineering, IIT Hyderabad*
[d] *ACCIS, University of Bristol, Queen's Building, University Walk, Bristol BS8 1TR, UK*
[e] *Bernal Institute, University of Limerick, Ireland.*

Abstract

Variable Angle Tow (VAT) laminates that generally exhibit variable stiffness properties not only provide extended design freedom, but also offer beneficial stress distributions. In this paper, the prospect of VAT composite panels with significantly reduced loss of in-plane compressive stiffness in the postbuckled state in comparison with conventional structures, is studied. Specifically, we identify that both thickness and local fiber angle variation are required to effectively define "buckle-free" panels under compression loading. In this work, the postbuckling behaviour of variable thickness VAT composite panels is analyzed using an efficient and robust semi-analytical approach. Most previous works on the postbuckling of VAT panels assume constant thickness. The additional benefits of tailoring thickness variation in the design of VAT composite panels are seldom studied. However, in the process of manufacturing VAT laminates, either by using the conventional Advanced fiber Placement (AFP) machine (tow overlap) or the newly developed Continuous

*Corresponding author
Email address: wuz12@cardiff.ac.uk; z.wu@tongji.edu.cn (Zhangming Wu)

Tow Shearing (CTS) process (tow shrink) thickness build-up is inevitable. The postbuckling optimization for the design of VAT layups is conducted by a two-level framework using lamination parameters as intermediate design variables. The objective is to determine optimal lamination parameters and thickness distributions for maximizing the axial compressive stiffness of VAT laminates that are loaded in the postbuckling regime. The thickness variation due to both manufacturing of VAT laminates and for where it is independent of manufacturing process are considered. In accordance with the first-level optimal postbuckling solutions in terms of lamination parameters, we investigate a practical "buckle-free" VAT panel using a blended layup configuration. This blended VAT panel consists of a piecewise combination of segmental CTS layers and constant-thickness VAT layers. The prospect of taking advantage of a benign combination of stiffness and thickness to improve the overall compressive strength of VAT panels is studied. Finally, the optimal results are analysed to provide insight into the manufacturing of VAT laminates using either the AFP or the CTS process for improved postbuckling stiffness under compression loading.

Keywords: Postbuckling, Optimization, Composite, Variable Angle Tow, Variable Thickness, Buckle-Free

1. Introduction

Laminated composite structures are increasingly used in the aviation and aerospace industry as primary load carrying components, due to their high strength-to-weight ratios and large stiffness tailoring flexibility. The design of lightweight aircraft structures is often driven by weight savings under a buckling strength criterion. For example, wing covers are normally designed to restrict the buckling occurrence with respect to an ultimate operating load [1]. Further weight savings can be achieved if composite structures are allowed to continuously operate into the nonlinear postbuckling regime. Composite panels usually suffer from a certain amount of loss of in-plane

stiffnesses after entering into the postbuckling state. This research attempts to suppress the loss of in-plane compressive stiffness of the postbuckled composite panels to a minimum level. In other words, we are aiming to design "Buckle-Free" composite panels, of which a high in-plane compressive stiffness is retained regardless of the structural operating state. A two-level optimization framework with a general variable stiffness tailoring approach is applied for the design of "Buckle-Free" composite panels.

The buckling of flat panels is associated with both a loss of in-plane stiffness and also growth of out-of-plane displacements. As buckling occurs, in-plane loads are redistributed to supported regions and are accompanied by an associated loss of in-plane stiffness. This phenomenon informs von Karman's effective width concept [53, 6]. Therefore, in a practical sense we can consider buckling as an in-plane load redistribution event. Our "Buckle-Free" concept exploits this interpretation of buckling by using a combination of thickness and stiffness tailoring to redistribute in-plane loads prior to buckling. Subsequently, if there is no further load-redistribution at the point of buckling (growth of out-of-plane displacements) then there will be no associated loss of in-plane stiffness and therefore the panel is effectively "Buckle-Free" in terms of in-plane load carrying capability. In other words, this "Buckle-Free" panel is able to continuously carry considerable loads, beyond the critical buckling point, without losing any stiffness.

Conventional straight-fiber laminates offer a limited tailoring option, by designing the stacking sequence with constant ply-angles along the thickness direction. The development of variable stiffness technology enables the stiffness properties of composite materials to vary from one point to another. As such, it offers a fully three-dimensional tailoring capacity. Numerous works have shown that structural performance can be significantly improved through optimizing the spatially point-wise stiffness variation. Variable stiffness structures can be achieved by either steering fibers in curvilinear paths (VAT plies) or by using an additional thickness variation. Early works consid-

ered the variable thickness approach. Capey [2] showed substantial increase of buckling load of isotropic plates made up of three strips, in which the outer strips are thicker than the central one. Biggers *et al.* [1, 3] applied an analogous tailoring configuration to laminated composite plates and obtained much larger improvement in buckling load. More recently, many papers have [4, 5, 6, 7, 8, 9] focused on the study of VAT composites that enable the tailoring of local directional properties of composite materials. Constant-thickness VAT plies are assumed in most works. However, thickness variation of VAT laminates is inevitable in the tow-steering manufacturing process, for example the tow overlaps and gaps induced by AFP (Automated Fiber Placement) machine, and the thickened tows in CTS (Continuous Tow Shearing) method. Such thickness changes in VAT laminates are strongly coupled with a particular manufacturing method, and therefore usually restricts the tailoring flexibility.

To minimise unnecessary design limitations, the thickness is allowed to independently vary in a point-wise manner across the planform of VAT composite plates in this work. The stiffness matrices of VAT panels at each point are defined in terms of lamination parameters and an independent thickness variable. In so doing, a general variable stiffness design philosophy is applied and the flexibility of stiffness tailoring achieves a maximum. Herein, stiffness tailoring is implemented through both local layup arrangement (thickness tailoring) and local placement of various orientation composite fibers across the planform of panels (VAT design). As a consequence, the membrane and bending stiffnesses of composite panels exhibit non-uniform distributions and can be locally optimized. In addition, the variable stiffness properties may give rise to benign redistributions of non-uniform in-plane stress resultants that can directly benefit the buckling and post-buckling strength substantially. This new design philosophy eventually enables us to achieve the "Buckle-free" composite panel design.

The nonlinear postbuckling analysis is a time-consuming process, in par-

ticular when a finite element model is applied. Therefore, there remains a need for tools that can rapidly and accurately predict the postbuckling response of laminated composite structures. Many previous works that developed semi-analytical modelling methods are usually the first choice for postbuckling optimization of composite structures, due to their high computational efficiency and physically intuitive insight. Most early works developed the analytical/semi-analytical postbuckling modellings based on the energy methods and considered various combined loading cases. Some semi-analytical postbucking approaches were inserted into gradient-based optimization routines to form integrated design packages or tools, such as POSTOP [10], PANDA2 [11], NLPANOPT [12, 13] and VICONOPT [14, 15]. These tools have been successfully applied to optimize the postbuckling behaviour of various thin-walled structural sections from metal or composite panels [16], to stiffened panels [10] and cylindrical panels [11] etc. Perturbation methods have also been often used to model the postbuckling behaviour of thin-walled structures to obtain asymptotic solutions (sometimes in closed-forms). Recently, some works successfully applied asymptotic perturbation models in the postbuckling optimization of composite structures. Wu *et al.* [17] derived explicit closed-form expressions with improved accuracy than Shen and Zhang's previous perturbation model [18, 19] for the postbuckling analysis of orthotropic composite plates. These formulae obtain the global optimal solutions for constant stiffness composite layups with either minimum end-shortening strains or minimum out-of-plane deflections. Henrichsen *et al.* [20] developed a novel Koiter's asymptotic method based finite element modelling approach and applied it in a gradient-based postbuckling optimization routine of composite panels. Raju *et al.* [21] applied a perturbation based asymptotic numerical method (ANM) to perform the postbuckling optimization of constant-thickness VAT panels using a two-level optimization framework, which is developed specifically for point-wise stiffness tailoring using lamination parameters [22].

Previously, an efficient Rayleigh-Ritz modelling was developed for the postbuckling analysis of VAT plates using a single mixed variational formula [6]. The postbuckling problem of composite plates with discontinuous thickness change is considered, in this work, for the design of blended VAT panels. The thickness of a blended VAT plate may not only vary in a continuous pattern caused by the manufacturing process of variable angle tows, but also involve discontinuous changes due to the piecewise placement of different number of VAT plies. The discontinuous thickness change results in stiffness discontinuities and variation of neutral axis position [23]. As a consequence, special care must be given to the formulation to accurately capture the true structural behaviour in the vicinity of the discontinuity. An early work by Benthem [24] presented a detailed analytical study on the buckling and initial postbuckling load-carrying capacity for various types of combined isotropic plate strips. The analytical solutions were obtained based on the von Kármán expressions and well-established formulae for the boundary conditions at various types of thickness changes, i.e. free edges, corners and transitions. Fox [25] performed the postbuckling analysis of plates with discontinuous thickness across the width, which exhibit substantially different behaviour from that of the equivalent uniformly thick plates. Coburn [23] recently proposed an element-wise semi-analytical (called SA-element) method to study the buckling of discontinuous stiffness beams and plates, in which the necessary continuities of displacement and rotation are enforced using penalty terms. Analogous to the SA-element method [23], blended VAT plates are also modelled by considering each portion with a different thickness variation pattern as an individual element.

The postbuckling optimization of VAT panels in this work aims to achieve the maximum overall stiffness [26] (the "buckle-free" concept) subject to a certain amount of compressive loading. The postbuckling optimization of VAT panels with variable thickness is conducted by a previously developed two-level framework [22]. At the first level, a general point-wise variable

stiffness pattern is optimized in terms of lamination parameters and independently varying thickness. B-spline functions are employed to define the spatial variation of lamination parameters and thickness. The B-spline formulated variation is determined by a prescribed knot vector and a set of control points, where the design variables are associated. The convex-hull property of B-Spline functions enable the entire distribution of lamination parameters to be constrained within the feasible region by applying the nonlinear constraints on the control points only [22]. At the second level, a genetic algorithm is applied to recover the optimal stiffness variation into realistic VAT layups. According to the optimal stiffness and thickness distribution obtained from the first-level procedure, a blended VAT design that consists of a piecewise combination of segmental CTS layers and constant-thickness VAT layers is proposed and optimized for the final "buckle-free" panel design.

The objective of this paper is to study a general stiffness tailoring concept through taking advantage of both thickness variation and variable angle tows in the design of composite structures. This general variable stiffness tailoring approach is implemented with the assistance of lamination parameters, and is applied to optimize the postbuckling load-carrying capacity of composite plates. The VAT panel designs that exhibit the distinct "Buckle-Free" attribute were obtained by the postbuckling optimization, and it also demonstrates the viability of applying our proposed general (material and thickness) varying stiffness concept. The novelties of this paper lie in the following aspects: (1) The proposed general variable stiffness tailoring concept; (2) The Buckle-Free panel design; (3) The establishment of element-wise postbuckling modelling; (4) The blended VAT composite laminates pattern.

The general stiffness tailoring approach that is characterized by lamination parameters is introduced in the next section. Section 3 presents the modelling work for the postbuckling analysis of VAT panels with discontinuous thickness changes. In section 4, the two-level postbuckling optimization

procedure for the VAT panels with independent variable thickness is described, including the design criteria and the optimization strategy. Section 5 presents the optimization results under different design assumptions and introduces the "buckle-free" blended VAT plate.

2. Variable Angle Tow Panels

2.1. Variable angle tow panels

VAT laminates allow the tailoring potential given by the local anisotropic (directional) properties of composite materials to be explored in the design of lightweight aircraft structures. To design VAT laminates, a mathematical description of tow-steering trajectories is necessary. A previous developed control-point based design scheme [22, 26, 27] is adopted to parameterize the fiber angle variation of VAT panels, as defined by the following equation,

$$\theta(x,y) = \sum_{m=0}^{M-1}\sum_{n=0}^{N-1} T_{mn} \cdot \prod_{m\neq i}\left(\frac{x-x_i}{x_m-x_i}\right) \cdot \prod_{n\neq j}\left(\frac{y-y_j}{y_n-y_j}\right) \tag{1}$$

where T_{mn} is the coefficient of each term in the series and is directly equal to the design variable (fibre angle) of each control point (x_m, y_n).

2.2. Thickness changes of VAT laminates

The development of advanced tow-steering manufacturing technologies enables the VAT placement across the plane of composite plies. VAT laminates are fabricated using embroidery-based machines [29], AFP [30, 31] and the newly developing CTS method [32, 33]. AFP applies in-plane bending deformation to steer the tows into curvilinear paths and is currently considered as the key enabling technology [32]. Two different ways have been used for the placement of variable angle tows over the plane of composite plies: the parallel and shifted methods [34]. The parallel method theoretically produces constant thickness VAT plies without tow gaps and overlaps.

However, it has not been widely used because of its limited manufacturing efficiency, restricted steering radius [35] and geometric singularity [36]. The shifted method that keeps tow trajectories parallel to the reference fiber path is much more efficient. However, as shown in Figure 1, the shifted method inevitably involves tow gaps, overlaps and other defects [33]. Tow overlaps result in local thickness build-up and localized resin pocket defect. Cutting the unnecessary part of tows reduces the occurrence of tow overlaps but also induces tow discontinuities [36].

Instead of bending the composite tows, the CTS technique applies in-plane shear deformation to continuously "shear" tow elements to produce curvilinear fibers [32]. The CTS method can avoid local fiber wrinkling or buckling that are often induced by an AFP manufacturing process with the in-plane bending method [35]. Since all fibers within each tow are aligned exactly to follow the prescribed curvilinear paths, tow gaps and overlaps can be avoided [35]. In addition, the CTS technique enables manufacturing of steering tows with smaller radius ($30mm$) than conventional AFP machines [32]. The width of the tow along the perpendicular direction of fibers (section B-B) shrinks after the tow element is sheared to a certain angle θ, as shown in the uppermost plot of Figure 1-(b). As a consequence, the fibers within a narrow tow are stacked and increase the thickness of tows. Considering that the fiber volume of the sheared tow element remains unchanged ($t_0 w_0 = t w_0 \cos\theta$), the thickness build-up of a CTS-manufactured variable angle tow is calculated by [33],

$$t = t_0 / \cos\theta \tag{2}$$

where t_0 and θ are the original tow thickness and the shear angle, respectively and w_0 is the original tow width. Note, θ herein refers to the shear angle, which is different with the fiber orientation angle when a non-zero rotation angle (ϕ) is applied [36]. Figure 1-(b) shows the CT scan image of the cross section along the width direction of a CTS panel, which approves Eq. (2) in predicting the thickness variation induced by the CTS process.

It can be seen that both AFP and CTS techniques induce certain thickness variation to VAT laminates during the tow-steering procedure. Such thickness changes highly depend on the distribution pattern of variable fiber angles, and consequently restrict the design flexibility of variable stiffness laminates. The AFP method often induces tow overlaps and tow gaps to VAT laminates, which cause irregular thickness build-up and local resin rich pocket, respectively. These defects lead to irregular local stiffness changes and eventually cause much difficulty to the numerical modelling and optimal design. CTS-manufactured VAT laminates have smooth thickness variation which is governed by Eq. (2). Substantial thickness build-up occurs for CTS laminate plies when large shear angles are applied. Previous works have shown that the compressive buckling strength of CTS panels can significantly benefit from the thickness build-up along the unloaded transverse edges [36, 37, 38].

2.3. General variable stiffness tailoring

A general variable stiffness tailoring design philosophy is proposed in this work to optimize the postbuckling behaviour of VAT panels. The tailoring concept herein allows the thickness of VAT laminates to independently vary in a point-wise manner. Lamination parameters are used to characterize the local directional properties of VAT composite layups. The use of lamination parameters not only reduces the number of design variables to a minimum, but also provides a full design space for the laminate configuration [39, 40]. Since only specially orthotropic laminates are considered at the first-level design process, there is no extension-shear coupling ($A_{16} = 0, A_{26} = 0$) and no flexural-twisting coupling ($D_{16} = 0, D_{26} = 0$). Therefore, only four lamination parameters (two in-plane and two out-of-plane) are needed to define the stiffness matrices of VAT laminates. The in-plane and bending stiffness matrices $A_{ij}(x, y), D_{ij}(x, y)$ are then expressed in terms of lamination parameters, an independent thickness variable and material invariants

U_1, U_2, U_3, U_4, U_5 [40] as,

$$\begin{bmatrix} A_{11}(x,y) \\ A_{22}(x,y) \\ A_{12}(x,y) \\ A_{66}(x,y) \end{bmatrix} = h(x,y) \begin{bmatrix} 1 & \xi_1^A(x,y) & \xi_2^A(x,y) & 0 & 0 \\ 1 & -\xi_1^A(x,y) & \xi_2^A(x,y) & 0 & 0 \\ 0 & 0 & -\xi_2^A(x,y) & 1 & 0 \\ 0 & 0 & -\xi_2^A(x,y) & 0 & 1 \end{bmatrix} \begin{pmatrix} U_1 \\ U_2 \\ U_3 \\ U_4 \\ U_5 \end{pmatrix} \tag{3}$$

$$\begin{bmatrix} D_{11}(x,y) \\ D_{22}(x,y) \\ D_{12}(x,y) \\ D_{66}(x,y) \end{bmatrix} = \frac{h(x,y)^3}{12} \begin{bmatrix} 1 & \xi_1^D(x,y) & \xi_2^D(x,y) & 0 & 0 \\ 1 & -\xi_1^D(x,y) & \xi_2^D(x,y) & 0 & 0 \\ 0 & 0 & -\xi_2^D(x,y) & 1 & 0 \\ 0 & 0 & -\xi_2^D(x,y) & 0 & 1 \end{bmatrix} \begin{pmatrix} U_1 \\ U_2 \\ U_3 \\ U_4 \\ U_5 \end{pmatrix} \tag{4}$$

where $\xi_{1,2}^A(x,y)$, $\xi_{1,2}^D(x,y)$ are the distribution functions of two in-plane lamination parameters and two out-of-plane lamination parameters, respectively. With the introduction of the independent thickness variation $h(x,y)$ in Eqs. (3) and (4), the flexibility of variable stiffness tailoring of VAT panels achieves a maximum. The four lamination parameters ($\xi_{1,2}^{A,D}$) are used to characterize the stiffness matrices of orthotropic laminates. The feasible region of these four coupled lamination parameters had been studied and defined mathematically in the previous works [7, 22].

Although the variable-stiffness variable-thickness composite laminates have been studied in previous works [41, 42], the design approach proposed in this paper based on lamination parameters is more general, and is able to give the global optimum. This proposed design approach enables a composite designer to simultaneously explore the benefits provided by the varying fiber orientation angles with independent thickness variation, by which outstanding structural attributes for composite structures are achieved. The "Buckle-Free" panel presented in this work is an example to demonstrate the

viability of applying this general variable stiffness tailoring concept in the postbuckling optimization of composite panels.

3. Theoretical Modelling for VAT Panels

3.1. Basic postbuckling model

The fundamental theory for the nonlinear postbuckling analysis of thin-walled composite panels is derived from the well-known von Kármán large deflection equations [43]. In previous works, an efficient semi-analytical modelling for the postbuckling analysis of VAT panels have been developed from a single mixed variational formula [52],

$$\begin{aligned}\boldsymbol{\Pi}^{*} = &-\frac{1}{2}\iint_{S}\left[a_{11}(x,y)(\Phi_{,yy})^{2}+2a_{12}(x,y)\Phi_{,xx}\Phi_{,yy}+a_{22}(x,y)(\Phi_{,xx})^{2}+\right.\\ &\left.a_{66}(x,y)(\Phi_{,xy})^{2}-2a_{16}(x,y)\Phi_{,yy}\Phi_{,xy}-2a_{26}(x,y)\Phi_{,xx}\Phi_{,xy}\right]dxdy\\ &+\frac{1}{2}\iint_{S}\left[D_{11}(x,y)(w_{,xx})^{2}+2D_{12}(x,y)w_{,xx}w_{,yy}+D_{22}(x,y)(w_{,yy})^{2}+\right.\\ &\left.4D_{66}(x,y)(w_{,xy})^{2}+4D_{16}(x,y)w_{,xx}w_{,xy}+4D_{26}(x,y)w_{,yy}w_{,xy}\right]dxdy\\ &+\frac{1}{2}\iint_{S}\left[\Phi_{,yy}(w_{,xx})^{2}+\Phi_{,xx}(w_{,yy})^{2}-2\Phi_{,xy}w_{,x}w_{,y}\right]dxdy\\ &+\int_{c_1}\left[M_{\nu 0}w_{,\nu}-(V_{z0}+M_{\nu s0,s})\,w\right]ds+\int_{c_2}\left[u_{0}N_{x\nu}+v_{0}N_{y\nu}\right]ds\end{aligned} \tag{5}$$

The Airy's stress function (Φ) and the out-of-plane displacement field (w) are expanded into series forms and substituting into this mixed variational functional Eq.(5), a basic postbuckling model for VAT panels is established [6, 27].

3.2. VAT panels with discontinuous thickness changes

To facilitate the thickness variation in variable stiffness tailoring, VAT panels with discontinuous thickness changes are considered in the postbuckling analysis. For simplicity, a blended (also called "tapered" [45]) VAT plate

made up of three segments (strips) in which the central part differs in thickness (number of plies) from the outer segments is proposed, as shown in Figure 2. This prototype of blended VAT plates is constructed through adding composite plies at outer segments and maintaining the fiber-continuity of the plies at the central region. By enforcing fiber continuity then tow (fiber) drop induced stress concentrations can be avoided [46]. Such blended composite panels can be manufactured by AFP machines, resin transfer molding (RTM) or by conventional hand layup method [1]. Previous works have shown that this type of thickness tailoring can provide a significant improvement of compressive buckling strength, even for isotropic plates [2].

Two different cross sections for the blended VAT panel are also illustrated in Figure 2. In the first case, the panel is symmetric with respect to the reference plane and therefore exhibits no bending-stretching coupling ($\mathbf{B} = 0$). However, the non-symmetric cross section with one curvilinear surface and one flat surface, as shown in the bottom plot of Figure 2, is more practical for the blended composite panels. If the reference plane of bending remains unchanged, the $\mathbf{B}$ matrix then becomes non-zero due to the non-symmetric cross section, and results in a certain amount of bending-stretching coupling. As a consequence, the VAT panel may not remain flat and could possess out-of-plane deflections before the buckling occurs depending on boundary conditions [23]. However, such pre-existing out-of-plane deflections during the pre-buckling state are relatively minor and can be neglected for most practical cases. This assumption enables the buckling problem of blended panels to be analyzed using a linear model [23]. The reduced bending stiffness (RBS) method [47, 48] is also applied to simplify the modelling of such blended VAT panels with non-symmetric cross sections. In the RBS method, the coupling matrix $\mathbf{b} = -\mathbf{A^{-1}B}$ in the partially inverted form of the constitutive equation [49] is ignored. In addition, an effective (reduced) bending stiffness matrix ($\mathbf{D}^* = \mathbf{D} - \mathbf{BA^{-1}B}$) is computed to replace the original bending stiffness matrix ($\mathbf{D}$) in the constitutive equation. Previous works

have shown that the RBS method can significantly reduce the modelling complexity and computational cost in the analysis of unsymmetrically laminated composites [47, 50], composite panels with discontinuous thickness changes [23, 51] and stiffened panels [52].

The basic postbuckling model derived from Eq. (5) can also be directly applied to solve the blended VAT-panel problems and give approximate solutions. Using C^∞ continuous shape functions to model a composite panel with discontinuous stiffness properties leads to inevitable errors to the resultant solutions in the vicinity of transitions between two different thicknesses. Coburn ([23], in chapter 4) presented a detailed analysis of such induced errors to the prebuckling and buckling results in terms of stresses, displacements and curvatures. A more accurate postbuckling model is therefore needed to capture the true discontinuous structural behaviours of blended VAT panels, particularly near the transition regions.

3.3. Boundary conditions

The whole VAT panel is simply-supported and subjected to a uniform displacement compressive loading ($x = \pm\frac{a}{2}$:$u = \mp\frac{\Delta_x}{2}$). For in-plane boundary conditions, the transverse edges are free to move but remain straight (denoted as *case C* in previous works [6, 21]).

At the transitions between two different thicknesses, the following boundary conditions need to be satisfied to ensure the geometric continuity [2, 24] (i and j denote two adjacent elements),

$$\begin{aligned} w_i &= w_j \\ \frac{\partial w_i}{\partial y_i} &= \frac{\partial w_j}{\partial y_j} \end{aligned} \tag{6}$$

In addition, the equality of the bending moment M_y and the continuity of the modified shear force $Q_y + \frac{\partial M_{xy}}{\partial x}$ [1] lead to another two natural boundary

[1] This is wrongly stated as $Q_y - \frac{\partial M_{xy}}{\partial x}$ in both refs. [2, 24]

conditions as,

$$\begin{aligned} -D_{22}^{*(i)}\frac{\partial^2 w_i}{\partial y_i^2} - D_{12}^{*(i)}\frac{\partial^2 w_i}{\partial x^2} &= -D_{22}^{*(j)}\frac{\partial^2 w_j}{\partial y_j^2} - D_{12}^{*(j)}\frac{\partial^2 w_j}{\partial x^2} \\ -D_{22}^{*(i)}\frac{\partial^3 w_i}{\partial y_i^3} - \left(D_{12}^{*(i)} + 4D_{66}^{*(i)}\right)\frac{\partial^3 w_i}{\partial x^2 y_i} &= -D_{22}^{*(j)}\frac{\partial^3 w_j}{\partial y_j^3} - \left(D_{12}^{*(j)} + 4D_{66}^{*(j)}\right)\frac{\partial^3 w_j}{\partial x^2 y_j} \end{aligned} \tag{7}$$

The boundary conditions associated with Airy's stress function to ensure the continuity of the in-plane normal force N_y, the shear force N_{xy} along the junctions are given by [24],

$$\begin{aligned} \frac{\partial^2 \Phi_i}{\partial x^2} &= \frac{\partial^2 \Phi_j}{\partial x^2} \\ \frac{\partial^2 \Phi_i}{\partial x \partial y_i} &= \frac{\partial^2 \Phi_j}{\partial x \partial y_j} \end{aligned} \tag{8}$$

To ensure the continuity of the normal strain ϵ_x and the strain compatibility $\frac{\partial \epsilon_x}{\partial y} - \frac{\partial \gamma_{xy}}{\partial x}$, we have another two boundary conditions for the Airy's stress function as,

$$\begin{aligned} a_{11}^{(i)}\frac{\partial^2 \Phi_i}{\partial y_i^2} + a_{12}^{(i)}\frac{\partial^2 \Phi_i}{\partial x^2} &= a_{11}^{(j)}\frac{\partial^2 \Phi_j}{\partial y_j^2} + a_{12}^{(j)}\frac{\partial^2 \Phi_j}{\partial x^2} \\ a_{11}^{(i)}\frac{\partial^3 \Phi_i}{\partial y_i^3} + (a_{12}^{(i)} + a_{66}^{(i)})\frac{\partial^3 \Phi_i}{\partial x^2 \partial y_i} &= a_{11}^{(j)}\frac{\partial^3 \Phi_j}{\partial y_j^3} + (a_{12}^{(j)} + a_{66}^{(j)})\frac{\partial^3 \Phi_j}{\partial x^2 \partial y_j} \end{aligned} \tag{9}$$

3.4. Element-wise postbuckling model

Herein, two different methods are implemented for the postbuckling analysis of blended VAT panels. One is based on the *superposition method*, in which additional terms for the central element are introduced to improve the modelling accuracy at junctions, and given as,

$$\Phi(\xi, \eta) = \Phi_0(\xi, \eta) + \Phi_1(\xi, \eta) + \Phi_s(\xi, \eta) \tag{10}$$

$$w(\xi, \eta) = w_0(\xi, \eta) + w_s(\xi, \eta) \tag{11}$$

where $\Phi_s(\xi,\eta)$ and $w_s(\xi,\eta)$ (the subscript or the superscript 's' indicates the local shape functions) are the additional terms, which are designed to capture the local structural behaviour. The terms $\Phi_s(\xi,\eta)$ and $w_s(\xi,\eta)$ are defined to be only non-zero at the central part of the blended VAT panels (Element-2 in Figure 2) as,

$$\Phi_s(\xi,\eta) = \begin{cases} \sum_{pq} \Phi_{pq}^{(s)} X_p(\xi) Y_q^{(s)}(\eta_1) & |y| \le \alpha b/2 \\ 0 & |y| > \alpha b/2 \end{cases} \tag{12}$$

$$w_s(\xi,\eta) = \begin{cases} \sum_{mn} W_{mn}^{(s)} X_m(\xi) Y_n^{(s)}(\eta_1) & |y| \le \alpha b/2 \\ 0 & |y| > \alpha b/2 \end{cases} \tag{13}$$

where $\eta_1 = 2y/(\alpha b) = \eta/\alpha$ is a local normalized coordinate for the central element along y axis and $\alpha = b_2/b$ is the normalized width for the central element with respect to the whole panel-width. The admissible shape functions $X_p(\xi)$ and $X_m(\xi)$ are required to satisfy the global boundary conditions for the normal stress (analogous to C-C, refer to Table 1) and the transverse displacement (S-S, refer to Table 1) respectively,

$$X_p(\xi) = (1-\xi^2)^2 L_p(\xi), \quad X_m(\xi) = (1-\xi^2) L_m(\xi) \tag{14}$$

where $L_p(\xi)$ and $L_m(\xi)$ are Legendre (orthogonal) polynomials. To ensure local continuity along the y directional boundaries of the central element, $Y_q^{(s)}(\eta_1)$ and $Y_n^{(s)}(\eta_1)$ are defined analogously to C-C boundary conditions,

$$Y_q^{(s)}(\eta_1) = (1-\eta_1^2)^2 L_q(\eta_1), \quad Y_n^{(s)}(\eta_1) = (1-\eta_1^2)^2 L_n(\eta_1) \tag{15}$$

As such, the continuity of deflection, rotation and in-plane stresses as defined in Eqs. (6) and (8) are ensured, respectively. Substituting stress resultants Eqs. (10) and (11) into the mixed variational functional Eq. (5), an improved postbuckling model for the blended VAT panel is derived. However, the modelling errors induced by C^∞ shape functions cannot be avoided in the

superposition method.

To overcome the discontinuity issue, an element-wise method that divides the blended VAT panel into elements at the locations of discontinuities is applied, as shown in the bottom plot of Figure 2. Each element is then considered as an independent plate, and modelled by separated shape functions with satisfying necessary boundary conditions and continuity constraints [2]. The mixed variational principle expressed in Eq. (5) is also computed individually in an element-wise manner. Additionally, penalty terms (or the Lagrangian Multipliers) are added into the whole functional to ensure the continuity of essential boundary conditions between two adjacent elements, as defined in Eqs. (6) and (8). The constraints for stress or moment equilibrium at transitions are not necessarily to be enforced in a weak-form based modelling procedure. For each element, Airy's stress function and out-of-plane deflection are defined individually and expanded into independent series as,

$$\Phi_j(\xi,\eta_1) = \Phi_0^{(j)}(\xi,\eta_1) + \sum_{p_j=0}^{P_j}\sum_{q_j=0}^{Q_j} \phi_{p_jq_j}^{(j)} X_{p_j}^{(j)}(\xi) Y_{q_j}^{(j)}(\eta_1) \tag{16}$$

$$w_j(\xi,\eta_1) = \sum_{m_j=0}^{M_j}\sum_{n_j=0}^{N_j} W_{m_jn_j}^{(j)} X_{m_j}^{(j)}(\xi) Y_{n_j}^{(j)}(\eta_1) \tag{17}$$

where index j denotes the j^{th} element and $X_{p_j}^{(j)}$, $Y_{q_j}^{(j)}$, $X_{m_j}^{(j)}$ and $Y_{n_j}^{(j)}$ are the polynomial shape functions for the j^{th} element. The boundary conditions for these shape functions are defined in accordance with the global and internal boundary conditions [23]. Table 1 lists both the global and internal boundary conditions for the stress and deflection shape functions of each element.

3.5. Model implementation

The thickness changes of blended VAT panels in our design are not significant at transitions. It was found that approximate stress fields given by a single Airy's stress function can also yield sufficiently accurate postbuck-

Table 1: Global and internal boundary conditions for the Airy's stress function Φ and the out-of-plane deflection function w at each element. S: Simply-supported; F: Free; C: Clamped.

	w		Φ	
	$X_{m_j}^{(j)}$	$Y_{n_j}^{(j)}$	$X_{p_j}^{(j)}$	$Y_{q_j}^{(j)}$
Element-1	S-S	S-F	C-C	C-F
Element-2	S-S	F-F	C-C	F-F
Element-3	S-S	F-S	C-C	F-C

ling solutions. Therefore, to reduce modelling complexity and computational costs, Airy's stress function still takes the form of Eq. (10) and the out-of-plane deflection function w is implemented either by the *superposition method* (Eq. (13)) or by the element-wise method (Eq. (17)). For the *superposition method*, substituting Eqs. (11) and (13) into the mixed variational functional Eq. (5), the following nonlinear algebraic equations are obtained for the postbuckling model:

$$
\begin{aligned}
&K_{pi}^{mm}\phi_p + K_{ki}^{mc}c_l + K_{ki}^{md}d_l + K_{rsi}^{mb}W_rW_s + K_{rsi}^{mbs}W_r^{(s)}W_s + K_{rsi}^{ms}W_r^{(s)}W_s^{(s)} = 0\\
&K_{pi}^{cm}\phi_p + K_{ki}^{cc}c_l + K_{ki}^{cd}d_l + K_{rsi}^{cb}W_rW_s + K_{rsi}^{cbs}W_r^{(s)}W_s + K_{rsi}^{cs}W_r^{(s)}W_s^{(s)} = F_{xi}\\
&K_{pi}^{dm}\phi_p + K_{ki}^{dc}c_l + K_{ki}^{dd}d_l + K_{rsi}^{db}W_rW_s + K_{rsi}^{dbs}W_r^{(s)}W_s + K_{rsi}^{ds}W_r^{(s)}W_s^{(s)} = F_{yi}\\
&K_{ri}^{bb}W_r + K_{ri}^{bs}W_r^{(s)} - K_{rpi}^{bm}W_r\phi_p - K_{rpi}^{bsm}W_r^{(s)}\phi_p -\\
&K_{rki}^{bc}W_rc_l - K_{rki}^{bsc}W_r^{(s)}c_l - K_{rki}^{bd}W_rd_l - K_{rki}^{bsd}W_r^{(s)}d_l = 0\\
&K_{ri}^{sb}W_r + K_{ri}^{ss}W_r^{(s)} - K_{rpi}^{sbm}W_r\phi_p - K_{rpi}^{sm}W_r^{(s)}\phi_p -\\
&K_{rki}^{sbc}W_rc_l - K_{rki}^{sc}W_r^{(s)}c_l - K_{rki}^{bsd}W_rd_l - K_{rki}^{sd}W_r^{(s)}d_l = 0
\end{aligned}
\tag{18}
$$

where $K_{pi}^{mm}, K_{rsi}^{ms}, \cdots, K_{rki}^{sd}$ represent various postbuckling stiffness matrices for a blended plate using the *superposition method*. The letters (b; s; m; c; d) in the superscript of each stiffness matrix (K) denote global bending, local bending for the central element, membrane, the boundaries of loaded edges and transverse edges, respectively.

Similarly, to implement an element-wise postbuckling modelling for blended VAT panels, Airy's stress function takes the form given in [6]. The out-of-plane deflection w is expanded individually for each element, according to the boundary conditions in Table 1,

$$\begin{aligned} w_1(\xi,\eta_1) &= \sum_{m_1=0}^{M_1}\sum_{n_1=0}^{N_1} W^{(1)}_{m_1n_1}(1-\xi^2)L_{m_1}(\xi)(1-\eta_1)L_{n_1}(\eta_1) \\ w_2(\xi,\eta_2) &= \sum_{m_2=0}^{M_2}\sum_{n_2=0}^{N_2} W^{(2)}_{m_2n_2}(1-\xi^2)L_{m_2}(\xi)L_{n_2}(\eta_2) \\ w_3(\xi,\eta_3) &= \sum_{m_3=0}^{M_3}\sum_{n_3=0}^{N_3} W^{(3)}_{m_3n_3}(1-\xi^2)L_{m_3}(\xi)(1+\eta_1)L_{n_3}(\eta_1) \end{aligned} \tag{19}$$

To ensure the continuity of each connecting boundary between elements, four additional penalty terms are added into the mixed variational functional as,

$$\Pi^{**} = \Pi^{*} + P^{(w)}_{12} + P^{(dw)}_{12} + P^{(w)}_{23} + P^{(dw)}_{23} \tag{20}$$

where $P^{(w)}_{12}, \cdots, P^{(dw)}_{23}$ are the additional penalty terms that are introduced to satisfy the out-of-plane deflection and rotation constraints of connecting boundaries given in Eq. (6). The numbers $1, 2, 3$ in the subscripts of the penalty terms denote each individual element, while the superscripts w and dw represent the deflection and rotation, respectively. The penalty terms are

expressed as integrals along the connecting boundaries [23],

$$
\begin{aligned}
P_{12}^{(w)} &= \frac{k_{12}^{(w)}}{2}\int_{-\frac{a}{2}}^{\frac{a}{2}}\left[\left(w_1-w_2\right)^2|_{y=y_{12}}\right]dx \\
P_{12}^{(dw)} &= \frac{k_{12}^{(dw)}}{2}\int_{-\frac{a}{2}}^{\frac{a}{2}}\left[\left(\frac{\partial w_1}{\partial y}-\frac{\partial w_2}{\partial y}\right)^2\Big|_{y=y_{12}}\right]dx \\
P_{23}^{(w)} &= \frac{k_{23}^{(w)}}{2}\int_{-\frac{a}{2}}^{\frac{a}{2}}\left[(w_2-w_3)^2|_{y=y_{23}}\right]dx \\
P_{23}^{(dw)} &= \frac{k_{23}^{(dw)}}{2}\int_{-\frac{a}{2}}^{\frac{a}{2}}\left[\left(\frac{\partial w_2}{\partial y}-\frac{\partial w_3}{\partial y}\right)^2\Big|_{y=y_{23}}\right]dx
\end{aligned}
\tag{21}
$$

where $k_{12}^{(w)},\cdots,k_{23}^{(dw)}$ are the coefficients with large values for the penalty terms. It was found that choosing the penalty coefficients sufficiently large (i.e. of order 10^8) ensures geometric compatibility (Eq. (19)).

Substituting the element-wise deflection shape functions w_i given by Eq. (19) into the modified mixed variational formula Eq. (20) and applying the Rayleigh-Ritz procedure, the following non-linear algebraic equations are obtained for the element-wise post-buckling model,

$$
\begin{aligned}
&K_{pi}^{mm}\phi_p+K_{ki}^{mc}c_l+K_{ki}^{md}d_l+\sum_{j=1}^{3}K_{rsi}^{mb_j}W_r^{(j)}W_s^{(j)}=0 \\
&K_{pi}^{cm}\phi_p+K_{ki}^{cc}c_l+K_{ki}^{cd}d_l+\sum_{j=1}^{3}K_{rsi}^{cb_j}W_r^{(j)}W_s^{(j)}=Fx_i \\
&K_{pi}^{dm}\phi_p+K_{ki}^{dc}c_l+K_{ki}^{dd}d_l+\sum_{j=1}^{3}K_{rsi}^{db_j}W_r^{(j)}W_s^{(j)}=Fy_j \\
&K_{ri}^{b_jb_j}W_r^{(j)}-K_{rpi}^{b_jm}W_r^{(j)}\phi_p-K_{rki}^{b_jc}W_r^{(j)}c_l-K_{rki}^{b_jd}W_r^{(j)}d_l+ \\
&\sum_{ef=12;23}\left(P_{ef}^{(w)}+P_{ef}^{(dw)}\right)=0 \quad j=1,2,3
\end{aligned}
\tag{22}
$$

where $K_{pi}^{mm},K_{ki}^{mc},\cdots,K_{rki}^{b_jd}$ represent various postbuckling stiffness matrices

for a blended panel modelled by an element-wise approach, in which the bending stiffness terms have been separated (denoted by b_j) for each element. The necessary penalty terms in the last three sets of non-linear algebraic equations in (22) are added to ensure geometric continuity.

4. Postbuckling Optimization

4.1. Postbuckling design of variable thickness VAT panels

This work aims to design well-behaved variable thickness VAT panels that are able to resist further load and retain the compressive stiffness after entering the postbuckling regime. The postbuckling performance of VAT panels is then optimized in terms of the end-shortening strain (ϵ_x) subjected to a fixed amount of applied load. The postbuckling solutions (non-linear equilibrium paths) were normalized with respect to the corresponding solutions of the quasi-isotropic plate. In so doing, the improvement of postbuckling load-carrying capacity in the design process is clearly quantified over the quasi-isotropic plate [53].

4.2. Two-level postbuckling optimization

The postbuckling optimization of variable thickness VAT panels is carried out using a two-level design framework [22], in which the lamination parameters are used as the intermediate design variables. At the first level, the optimal variable stiffness distribution that gives the maximum overall stiffness is determined using a gradient-based mathematical programming routine. At the second level, a well selected VAT panel in terms of stacking sequence, fiber angle variation of each ply and the blended panel construction pattern (if necessary) is decided in accordance with the optimal thickness variation. Lastly, a GA (Genetic Algorithm) based optimizer is applied to obtain the varying fiber orientations and other design parameters to realize the blended VAT panel design from the target stiffness variation.

As defined in Eqs. (3) and (4), the general variable stiffness is achieved by designing the distributions of four lamination parameters and independent thickness variation. Herein, a control-point based design scheme and B-spline functions, as illustrated in Figure 3, are employed to define the spatial variations of lamination parameters and panel-thickness [22]. The major reason for choosing B-spline functions is their strong convex hull property, which enables the entire distribution of the lamination parameters to be constrained within the feasible region only via the control points. When the lamination parameters and thickness are only varying along one principal direction (for example, the y-axis in this work), each variation is defined using a B-spline function as,

$$\begin{aligned} y(\bar{v}) &= \sum_n B_n^{(y)} N_n^{(k)}(\bar{v}) \\ \xi_{1,2}^{A,D}(\bar{v}) &= \sum_n \Gamma_n^{(\tau)} N_n^{(k)}(\bar{v}) \\ h(\bar{v}) &= \sum_n h_n N_n^{(k)}(\bar{v}) \end{aligned} \tag{23}$$

The first-level postbuckling optimization of variable thickness VAT panels is subsequently formulated as,

$$\begin{aligned} \textbf{min} \quad & \epsilon_x^o(\Gamma_{mn}^{(\tau)}, h_{mn}) \\ \textbf{subjected to:} \quad & -1 \leqslant \Gamma_{mn}^{(\tau)} \leqslant 1 \\ & g_i(\Gamma_{mn}^{(\tau)}) \leqslant 0 \\ & h_L \leq h_{mn} \leq h_U \\ & \frac{1}{ab}\int_{-a/2}^{a/2}\int_{-b/2}^{b/2} h(x,y)dxdy - h_0 \leq 0 \end{aligned} \tag{24}$$

where $\Gamma_{mn}^{(\tau)}$ is the lamination parameters at each point P_{mn}, $g_i(\Gamma_{mn}^{(\tau)})$ are the nonlinear constraint functions that define the feasible region of these four lamination parameters [22]. h_L and h_U are the lower and upper bounds

of the thickness variation. The last equation ensures the panel mass and equivalent distributed uniform thickness of the VAT panel does not exceed that of the baseline panel with constant thickness (h_0) in the design process. In fact, for the optimal results of variable thickness VAT panels, the panel mass and equivalent distributed uniform thickness always remain the same with that of the baseline panel (ultimate use of materials).

In the second level optimization process, a realistic VAT layup is retrieved to closely match the target variable stiffness distribution obtained from the first-level design process. A laminate design pattern with a well chosen stacking sequence with appropriate variation of each VAT layer is first evaluated. Each VAT layer is parameterized by the fibre angles defined at a set of control points. A smooth nonlinear variation (NLV) of fibre orientation angles over the plate domain is generated using Lagrangian polynomials, as given in Eq. (1). Subsequently, a GA is used to determine the fibre orientation angles at all the control points of each VAT layer.

In the design of constant thickness VAT panels, symmetrical and balanced stacking sequence is mostly used. For example, a 16-layer laminate $[\pm\theta_1/\pm\theta_2/\pm\theta_3/\mp\theta_4]_s$ possesses four VAT design layers, $\theta_1(x,y), \cdots, \theta_4(x,y)$. To design the variable thickness VAT panel, a particular blended laminate pattern needs to be decided upon in advance, and the design is normally based on the thickness variation. In this work, the AFP-machined constant thickness layers and CTS-manufactured variable thickness layers are combined to construct the blended VAT panel.

The fitness function of second level optimization is expressed as a mean value of the least square distance between the obtained stiffness variation and the target stiffness variation at a large number of grid points over the

plate domain [22, 53].

$$
\begin{aligned}
\textbf{min} \quad & \Delta_{A,D} = \frac{1}{N_p}\sum_{p}\Delta_{A,D}^{(p)} \\
& \Delta_{A,D}^{(p)} = \left[\sum_{ij} w_{ij}^{A}\left(A_{ij}-\tilde{A}_{ij}\right)^2 + \sum_{ij} w_{ij}^{D}\left(D_{ij}-\tilde{D}_{ij}\right)^2\right]_{(p)} \\
& \qquad (ij = 11, 12, 22, 66) \\
& [A_{ij}, D_{ij}] \leftarrow [\xi_{1,2}^{A,D}, h] \leftarrow \left[T_1^k, \cdots, T_n^k, \cdots, T_N^k\right] \\
\textbf{subjected to:} \quad & -\pi/2 \leqslant T_n^k \leqslant \pi/2
\end{aligned}
\tag{25}
$$

where the letter (p) in the superscript or subscript denotes a particular grid point. The total number of grid points (N_p) is chosen to be $100 \sim 300$ for one-dimensional design and $1000 \sim 2000$ for two-dimensional design. T_n^k is the fibre angle at the control point for the k-th ply and w_i^A and w_i^D are the weights to distinguish the relative importance between the in-plane stiffness (A_{ij}) and the out-of-plane stiffness (D_{ij}). Due to the difference of the orders of magnitude between (A_{ij}) and (D_{ij}), w_{ij}^A and w_{ij}^D are chosen to be 1 and $10^3 \sim 10^5$ (depending on the laminate configuration), respectively. In the GA optimization routine, the population size was set to be at least $20 \sim 30$ times the number of design variables, while the number of generations was $50 \sim 100$ depending on the population size. The crossover and mutation probabilities were chosen to be 0.7 and 0.04.

5. Results and Discussion

This section presents the optimization results of variable thickness VAT panels that possess the maximum overall compressive stiffness using the two-level design framework. In order to study the effect of thickness variation in the postbuckling design of VAT panels, three different cases of thickness variation are considered in this work: constant thickness, CTS-induced thick-

ness build-up and independent thickness variation. Lastly, we demonstrate a number of VAT-panel designs that possess the distinct "Buckle-Free" feature.

The lamina properties of the MTM49-3/T800 composite prepreg used in this work are given by $E_1 = 163$ GPa, $E_2 = 6.8$ GPa, $G_{12} = 3.4$ GPa, ν_{12}= 0.28. The length and width of VAT panels are $a = 0.5m$ and $b = 0.5m$, respectively. Ply thickness is 0.13mm. The thickness of the baseline VAT panel (with 16 plies) is 2.1 mm.

To validate the analytical postbuckling modelling for VAT panels with discontinuous thickness changes, in particular the blended VAT panels, finite element analysis was carried out using ABAQUS. A subroutine was developed to generate the elements with independent fiber orientations and independent thickness variations. Each element was assumed to have a constant fiber orientation and a separated thickness value. For the purpose of efficiency, the S4 shell element was chosen to discretize the VAT panel and a mesh density of 40×40 was used to achieve a desired accuracy. The accuracy of using S4 shell elements to model the postbuckling behaviour of VAT panels with discontinuous thickness changes was also validated against the results given by a full 3D finite element model (C3D8R). A small imperfection in the form of the first buckling mode shape and a magnitude of 1% of the plate thickness is imposed to each finite element model (FEM). The nonlinear postbuckling equilibrium paths are traced using the Riks method in Abaqus.

The optimal layups with maximum overall stiffness may be different when the level of axial compressive load N_{x0} varies. In this work, the value of axial load N_{x0} is fixed to be three times that of the critical buckling load ($3N_{iso}$) of an equivalent quasi-isotropic laminate. At the first level optimization procedure, the optimal variable stiffness distribution that gives the maximum postbuckling performance is determined first in terms of lamination parameters and thickness variation. The design parameters are associated with a set of uniformly distributed control points, and uniform quadratic B-spline basis functions are used to construct the variation of

lamination parameters and thickness. Since the postbuckling problem studied herein is symmetrical with respect to the boundary conditions, geometry and loading conditions, the distribution of lamination parameters and thickness is designed to be doubly symmetric for the two dimensional design $\xi_{1,2}^{A,D}(x,y) = \xi_{1,2}^{A,D}(|x|,|y|)$, $h(x,y) = h(|x|,|y|)$, and symmetric for the one dimensional design $\xi_{1,2}^{A,D}(y) = \xi_{1,2}^{A,D}(|y|)$, $h(y) = h(|y|)$. The second level optimization procedure for retrieving the realistic laminate layups from the target stiffness variation depends on the choice of the VAT laminate configuration for each different case study.

In this work, the optimal VAT-panel designs that give the maximum overall stiffness are obtained using different configurations of varying fiber angles and variable thickness. Table 2 lists the obtained VAT panels and their corresponding design parameters of VAT and variable thickness configurations. The improvement of each VAT-panel design with respect to overall stiffness compared to the $[\pm 45/0_6]_s$ layup is also given. The following subsections present the analysis of each VAT-panel design in details.

Table 2: Optimal design of general variable stiffness panels with respect to different configurations of VAT and thickness variation

Panel No.	VAT	Thickness	h_L	h_U	N_1 [a]	N_2 [b]	Improvement
CTS-1	CTS	$t_0/\cos(\theta)$	h_0	$3.86h_0$	-	1×3	17%
CTS-2	CTS	$t_0/\cos(\theta)$	h_0	$3.86h_0$	-	1×5	22.8%
VAT: #1	NLV	Constant	h_0	h_0	3×3	-	16%
VAT: #2	B-spline	Constant	h_0	h_0	7×7	-	24%
VAT: #3	B-spline	B-spline	$0.9h_0$	$4h_0$	1×7	1×7	31.2%
VAT: #4	B-spline	B-spline	$0.7h_0$	$4h_0$	1×7	1×7	48.8%
VAT: #5	B-spline	B-spline	$0.5h_0$	$4h_0$	1×7	1×7	55.5%
VAT: #6	B-spline	B-spline	$0.25h_0$	$4h_0$	1×7	1×7	62.1%
VTHC: #5	Constant	B-spline	$0.5h_0$	$4h_0$	-	1×7	50.2%

[a] The number of control points used for the variation of lamination parameters.
[b] The number of control points used for the thickness variation (for CTS, refer to the number of control points for nonlinear variation of fiber angles).

5.1. VAT panels with constant thickness

The optimal VAT layups with constant thickness that give maximum overall compressive axial stiffness (minimum end-shortening strain) are determined first and studied. For the constant thickness design, the design variables and corresponding constraints associated with thickness in the optimization problem Eq. (24) are eliminated. The postbuckling equilibrium paths for the optimized straight-fiber laminates and constant thickness VAT panels are compared and illustrated in Figure 4. The layup $[\pm 45/0_6]_s$ gives the minimum end-shortening strain among the constant stiffness laminates. VAT panel #1 is the optimal design obtained using a direct GA approach [26], while VAT panel #2 is the optimal result obtained from the first-level optimization procedure (in terms of two-dimensional distributions of lamination parameters). The result given by VAT panel #2 is approximately the global optima for the postbuckling behaviour design of constant-thickness variable stiffness panels. Compared to the best design of the straight-fiber laminate $[\pm 45/0_6]_s$, the VAT panel #1 shows 16% improvement and VAT panel #2 shows 24% improvement for the overall compressive stiffness. The VAT panels (#1 and #2) also show 71% and 51% increases on the critical buckling load, respectively.

The distributions of the four lamination parameters defined by 7×7 control points based B-spline functions for the VAT panel #2 are plotted in Figure 5. The realistic VAT layup is retrieved from this target lamination parameters distribution using a 3-by-3 control points based NLV fiber-angle design scheme, which had been presented in previous works [21, 9, 38]. It was revealed that the improvement of postbuckling performance (overall axial stiffness) for the constant thickness VAT panels mainly benefits from the variable stiffness induced stress re-distribution [26]. In addition, a large amount of 0-deg fibers [1, 9, 26] placed near the edges of the inner layers of VAT panels is also an essential factor for achieving a high prebuckling and postbuckling axial compressive stiffness.

5.2. CTS panels with edge thickness build-up

This section studies the variable stiffness and thickness build-up benefits offered by the CTS-manufactured composite plies in the postbuckling behaviour optimization. Currently, the CTS technique allows tows to be steered in one direction [32], and the thickness build-up of CTS layers is governed by Eq. (2). The critical buckling load of VAT panels can be improved significantly when CTS plies are used and optimized [36, 37]. However, such CTS panels with thick transverse edges often have quite poor axial compressive stiffness [6, 38]. According to a previous study [6], 0-deg plies placed at the inner layers result in a high axial compressive stiffness for composite panels. Therefore, a particular type of CTS laminate layup $[\pm\theta_1(y)/0_n]_s$ is employed in the postbuckling optimization for maximizing the overall compressive stiffness. In this CTS layup $[\pm\theta_1(y)/0_n]_s$, $\theta_1(y)$ is a CTS layer with the nonlinear variation of fiber angles only along y direction, which is defined by Eq. (1) using $3 \sim 5$ control points. The n in the layup $[\pm\theta_1(y)/0_n]_s$ denotes the number of 0-deg plies that are placed in the inner layers and are chosen to be $3 \sim 5$ in the laminate design. A standard GA routine is then used to determine the CTS tow trajectory and the number of 0-deg plies. In addition, a penalty term is added to the objective function to ensure the mass (average thickness) of the CTS panel does not exceed that of the baseline panel (h_0) in the optimization process. The optimization problem for the CTS panels is then formulated as,

Minimize:

$$\epsilon_x(\mathbf{x})/\epsilon_x^{iso} + \lambda \max(0, g(\mathbf{x}))^2 \tag{26}$$

Design Variables:

$$\mathbf{x}: \quad [T_0 \dots T_m \dots T_M; n] \;\; (M = 3 \text{ or } 5 \text{ for } \theta_1(y)) \tag{27}$$

subject to:

$$\begin{aligned} & 3 \leq n \leq 5 \\ & -5\pi/12 \leq T_m \leq 5\pi/12 \ \ (m = 1...3 \text{ or } 5) \\ & g(\mathbf{x}) : \frac{1}{ab}\int_{-a/2}^{a/2}\int_{-b/2}^{b/2} h(y)dxdy - h_0 \leq 0 \end{aligned} \tag{28}$$

where $\lambda, g(\mathbf{x})$ are the penalty coefficient and mass constraint function, respectively. Due to the CTS manufacturing limitation, the largest fiber orientation angle needs to be restrained less than $75°(5\pi/12)$. Figure 4 illustrates two optimized CTS panels (denoted as CTS-1 and CTS-2) for the minimum end-shortening strain when the external axial compressive loading is $N_x = 3N_{iso}$. The CTS-1 and CTS-2 panels are the optimal results using 3 control points and 5 control points for θ_1, respectively. Also, the number of 0 degree layers was chosen to be 4 in the layup $[\pm\theta_1/0_n]_s$ for both panels. Compared to the layup $[\pm 45/0_6]_s$, CTS-1 and CTS-2 panels achieve 17% and 22.8% improvement on the overall compressive stiffness, respectively. These results are also close to the optimal design of constant thickness VAT panels (#1 and #2) with two dimensional nonlinear variation of fiber angles. Figure 7 shows the fiber angles at control points and the tow trajectories for the CTS layers of each panel design. No further improvement in optimal postbuckling solutions for minimizing the end-shortening strain were found by either increasing the nonlinearity of fiber angle variation (more control points) or increasing the use of CTS layers in the layup. Therefore, the benefit purely given by the CTS plies is limited for the postbuckling behaviour design, partially because of the strong coupling defined in Eq. (2) between the thickness build-up and the fiber variation angles.

5.3. VAT panels with independent thickness variation

This section presents the optimal postbuckling designs for VAT panels with independent thickness variation, which provides the capability of gen-

eral variable stiffness tailoring. The postbuckling optimization problem with the general variable stiffness tailoring has been expressed in Eq. (24). The stiffness variation is defined in terms of four lamination parameters ($\xi_{1,2}^{A,D}$) and a thickness variable associated with each control point of the B-spline functions. Firstly, for the purpose of simplicity, one dimensional stiffness variation along y direction (with 7 control points defining the B-spline function) is allowed in the postbuckling optimization. Figure 7 illustrates different one-dimensional optimal postbuckling results (from VAT panels #3 to #6) that are obtained by setting different ranges of thickness variation. The upper bound of the thickness variation is set to be $h_U = 4h_0$, which is the maximum thickness build-up given by a CTS-manufacturing lamina with 75° shear angle. It was found that the thickness variation never exceeds the upper bound limit h_U in the optimization process. The VAT panels #3, #4, #5 and #6 are the optimal results when the lower bound of thickness variation is chosen to be $h_L = 0.9h_0, 0.7h_0, 0.5h_0$ and $0.25h_0$, respectively. From the postbuckling results shown in Figure 7 for the VAT panels #3 to #6, it can be seen that the postbuckling performance (overall axial stiffness) of the VAT panels can be substantially improved through inducing an independent thickness variation in the variable stiffness design.

An optimal panel with constant fiber angles and independent thickness variation is also obtained and denoted as VTHC #5 in Figure 7. The lower limit of thickness variation for VTHC #5 is set to be $h_L = 0.5h_0$ in the optimization process, which is the same with that of VAT panel #5. Compared with the structural behaviour of VAT panel #5, the VTHC #5 gives a very similar prebuckling and buckling behaviour but slightly lower postbuckling stiffness. This result clearly shows that an independent thickness tailoring is vital important for variable stiffness panels to gain a large compressive strength (both prebuckling and postbuckling). It was also found that the thickness variation profiles of VAT #5 and VTHC #5 are very similar to each other. The use of curvilinear fibers (variable angle tow) in VAT

#5 further improves the postbuckling stiffness, and eventually achieves the "Buckle-Free" design.

Moreover, the reduction in axial compressive stiffness of VAT panels #4 to #6 after entering the postbuckling regime is extremely low. The critical buckling points for the VAT panels #4 to #6 become less clear and are denoted by small circles in Figure 7. Therefore, the "Buckle-Free" design concept is eventually achieved. These results (VAT panels #3 to #6) also indicate that substantial benefits are received in the postbuckling behaviour design of VAT panels through general stiffness tailoring. Nevertheless, the VAT panel #6 is already approaching an ideal "Buckle-Free" panel design. VAT panels #4 to #6 are the optimal results from the first-level optimization process, of which only the variable stiffness distributions are given. For example, the stiffness variation of VAT panel #5 is given by the four lamination parameters ($\xi_{1,2}^{A,D}$) variations as shown in Figure 8 and a thickness variation along the y direction as given in Figure 9.

5.4. Blended VAT panels

In this section, a blended panel design scheme is considered and optimized to match the target stiffness distribution of VAT panel #5 that is obtained from the first-level optimization process. According to the type of thickness variation of VAT panel #5 given in Figure 9, the panel can be split into three parts that consist of one constant thickness central element and two outer elements with a large amount of thickness build-up. It was also noticed that the thickness variation pattern at the outer regions in Figure 9 is similar to the thickness build-up of a CTS laminate with large shear angles along edges. Therefore, a blended panel design scheme with 8 AFP-manufacturing constant thickness plies ($[\pm\theta_1^{\mathrm{AFP}}]_{2s}$) over the entire plate and 8 segmentally placed CTS composite plies at the outer regions ($[\pm\theta_2^{\mathrm{CTS}}]_{2s}$) is designed, as illustrated in Figure 10. The width ratio (α) of the central element is determined first from the thickness variation of VAT panel #5, that is $\alpha = b_2/b = 0.5586$ for this case. Subsequently, the second-level optimization

process as stated in Eq. (25) is carried out to determine the optimal fiber angles at the control points prescribed for the AFP layers ($\pm\theta_1$) and the CTS layers ($\pm\theta_2$). The second-level optimization solution enables the blended VAT panel to possess the closest stiffness variation to that of the VAT panel #5. Figure 11 shows the optimal results for the tow (fiber) trajectories of the AFP layers and CTS layers, which are both varying along y direction and are characterized by 5 and 3 control points, respectively. As shown in Figure 10, the constant-thickness AFP layers cover the entire panel, while CTS layers only placed at two outer regions for the blended VAT panel. The large axial compressive stiffness of this blended VAT panel benefits from a large amount of 0-deg fiber placement at the outer regions (θ_1 in Figure 11) and the edge thickness build-up pattern given by the segmental CTS layers.

The postbuckling behaviour of this optimized blended VAT panel is illustrated in Figure 12. Compared with the FEM result, the basic postbuckling model using single shape functions is unable to accurately capture the postbuckling behaviour of the blended VAT panel. The proposed element-wise postbuckling model as given in Eq. (22) yields an accurate result, as denoted by the solid green line in Figure 12. The postbuckling performance (overall axial stiffness) of this blended VAT panel is lower than the postbuckling result given by the target VAT panel #5. This reduction occurs mainly because the stiffness variation (in particular the thickness variation) of VAT panel #5 can not be matched exactly using such a blended VAT design. Nevertheless, the blended VAT panel that was obtained still demonstrates a distinct "Buckle-Free" feature.

6. Conclusion

A general variable stiffness tailoring approach in the postbuckling behaviour design of VAT panels has been developed, and is used to identify a "Buckle-Free" design concept. The general variable stiffness distribution is defined by B-spline functions using lamination parameters and an indepen-

dent thickness variable at each control point. Postbuckling optimization is carried out using a two-level optimization framework. To retrieve realistic laminates, a blended VAT panel design scheme that consists of a mixture of constant-thickness VAT layers and segmental placed CTS layers is proposed. It is then used to design the "Buckle-Free" composite panels from the target optimal stiffness variation. In order to improve modelling accuracy, an element-wise postbuckling model is developed to capture the nonlinear behaviour of blended VAT panels. The element-wise postbuckling model for VAT panels with discontinous thickness changes is validated by FEM results using Abaqus. In summary, the general variable stiffness tailoring approach with the two-level optimization framework and the blended VAT scheme enable the distinct design of "Buckle-Free" panels to be achieved.

From the optimal results, the benefits of using variable angle tows (VAT) with independent thickness variation are quantified for an enhanced axial compressive stiffness of composite panels that are loaded in the postbuckling regime. It was found that 0-deg fiber placement and significant thickness build-up at transversely supported regions of composite panels are the essential factors to achieve a high axial compressive stiffness. Guidelines are also provided for designers to achieve composite panels with high axial compressive stiffness.

Acknowledgments

The first author wish to sincerely acknowledge the financial support from China's 1000 Young Talent Programme and the Strathclyde Chancellor's Fellowship (University of Strathclyde, Scotland). All authors would like to acknowledge EPSRC, Airbus and GKN for supporting this research under the project ABBSTRACT2 (EP/H025898/1). Weaver would like to thank SFI (Science Foundation Ireland) for funding under its Research Professor programme.

References

[1] S. B. Biggers, S. Srinivasan, Compression buckling response of tailored rectangular composite plates, AIAA journal 31 (3) (1993) 590 – 596.

[2] E. C. Capey, The buckling under longitudinal compression of a simply supported panel that changes in thickness across the width, Ministry of Supply, Aeronautical Research Counci [C.P. No. 235] (1956) 1 – 36.

[3] M. G. Joshi, S. B. Biggers, Thickness optimization for maximum buckling loads in composite laminated plates, Composites Part B: Engineering 27 (2) (1996) 105 – 114.

[4] Z. Gürdal, B. Tatting, C. Wu, Variable stiffness composite panels: Effects of stiffness variation on the in-plane and buckling response, Composites Part A: Applied Science and Manufacturing 39 (5) (2008) 911 – 922.

[5] Z. Wu, G. Raju, P. M. Weaver, Buckling analysis of vat plate using energy method, 53rd AIAA/ASME Structures, Structural Dynamics and Materials Conference, (2012), AIAA 2012-1463.

[6] Z. Wu, G. Raju, P. M. Weaver, Postbuckling analysis of variable angle tow composite plates, International Journal of Solids and Structures 60 (0) (2013) 163 – 172.

[7] Z. Wu, G. Raju, P. M. Weaver, Feasible region of lamination parameters for optimisation of variable angle tow (VAT) composite plates, 54rd AIAA/ASME/ASCE/AHS/ASC Structures, Structural Dynamics and Materials Conference, (2013), AIAA 2013-1481.

[8] B. H. Coburn, Z. Wu, P. M. Weaver, Buckling analysis of stiffened variable angle tow panels, Composite Structures 111 (2014) 259 – 270.

[9] G. Raju, S. White, Z. Wu, P. M. Weaver, Optimal postbuckling design of variable angle tow composites using lamination parameters, 56th AIAA/ASME/ASCE/AHS/ASC Structures, Structural Dynamics and Materials Conference, AIAA SciTech Forum, (2015), AIAA 2015-0451.

[10] S. B. Dickson, J. N.; Biggers, Postop: Postbuckled open-stiffener optimum panels - theory and capability, NASA/CR-172259 (January, 1984) 1–39.

[11] D. Bushnell, Optimization of composite, stiffened, imperfect panels under combined loads for service in the postbuckling regime, Computer Methods in Applied Mechanics and Engineering 103 (1-2) (1993) 43 – 114.

[12] C. A. Perry, Z. Gürdal, J. H. Starnes, Minimum-weight design of compressively loaded stiffened panels for postbuckling response, Engineering Optimization 28 (3) (1997) 175–197.

[13] F. Stoll, Z. Gürdal, J. H. Starnes, A method for the geometrically nonlinear analysis of compressively loaded prismatic composite structures, NASA/CR 2002- 211919 (February 1991) 1–14.

[14] M. Lillico, R. Butler, G. Hunt, A. Watson, D. Kennedy, F. Williams, Analysis and testing of a postbuckled stiffened panel, AIAA Journal 40 (5) (2002) 996 – 1000.

[15] W. Liu, R. Butler, A. Mileham, A. Green, Bilevel optimization and postbuckling of highly strained composite stiffened panels, AIAA Journal 44 (11) (2006) 2562 – 2570.

[16] D. K. Shin, Z. Gürdal, J. O. Hayden Griffin, Minimum weight design of laminated composite plates for postbuckling performance, Applied Mechanics Reviews 44 (11S) (1991) S219–S231.

[17] Z. Wu, G. Raju, P. M. Weaver, Analysis and design for the moderately deep postbuckling behavior of composite plates, Journal of Aircraft 1 (1) (2016) 1 – 9.

[18] S. Hui-shen, Z. Jian-wu, Perturbation analyses for the postbuckling of simply supported rectangular plates under uniaxial compression, Applied Mathematics and Mechanics 9 (1988) 793–804.

[19] J. Zhang, H. Shen, postbuckling of orthotropic rectangular plates in biaxial compression, Journal of Engineering Mechanics 117 (5) (1991) 1158–1170.

[20] S. R. Henrichsen, P. M. Weaver, E. Lindgaard, E. Lund, Post-buckling optimization of composite structures using koiter's method, International Journal for Numerical Methods in Engineering 108 (8) (2016) 902 – 940.

[21] Z. Wu, G. Raju, P. M. Weaver, Optimal postbuckling design of variable angle tow composites using lamination parameters, Journal of Aircraft (2017) 1 – 9.

[22] Z. Wu, G. Raju, P. M. Weaver, Framework for the buckling optimization of variable-angle tow composite plates, AIAA Journal 53 (12) (2015) 3788 – 3804.

[23] B. H. Coburn, Buckling of stiffened variable stiffness panels, Ph.D. thesis, University of Bristol, UK (2015).

[24] J. P. Benthem, The buckling under longitudinal compression of a simply supported panel that changes in thickness across the width, Nat. Aero Res. Inst., Amsterdam NLL-TR S539 (1959) 1–25.

[25] W. Fox, J. Rhodes, Post-buckling behaviour of plates with discontinuous change of thickness, International Journal of Mechanical Sciences 19 (10) (1977) 603 – 618.

[26] Z. Wu, P. M. Weaver, G. Raju, Postbuckling optimisation of variable angle tow composite plates, Composite Structures 103 (2013) 34 – 42.

[27] Z. Wu, P. M. Weaver, G. Raju, B. C. Kim, Buckling analysis and optimisation of variable angle tow composite plates, Thin-Walled Structures 60 (0) (2012) 163 – 172.

[28] B. H. Coburn, P. M. Weaver, Buckling analysis, design and optimisation of variable-stiffness sandwich panels, International Journal of Solids and Structures 96 (2016) 217 – 228.

[29] P. M. Weaver, K. D. Potter, K. Hazra, M. A. Saverymuthapulle, M. T. Hawthorne, Buckling of variable angle tow plates: from concept to experiment, 50th AIAA/ASME/ASCE/AHS/ASC Structures, Structural Dynamics, and Materials Conference, Structures, Structural Dynamics, and Materials and Co-located Conferences, (2009), AIAA 2009-2509.

[30] Z. Gürdal, B. F. Tatting, K. C. Wu, Tow-placement technology and fabrication issues for laminated composite structures, 46th AIAA/ASME/ASCE/AHS/ASC Structures, Structural Dynamics and Materials Conference, (2005), AIAA 2005-2017.

[31] A. W. Blom, P. B. Stickler, Z. Gurdal, Design and manufacture of a variable-stiffness cylindrical shell, SAMPE Europe Conference and Exhibition, 2012.

[32] B. C. Kim, P. M. Weaver, K. Potter, Manufacturing characteristics of the continuous tow shearing method for manufacturing of variable angle tow composites, Composites Part A: Applied Science and Manufacturing 61 (2014) 141–151.

[33] B. C. Kim, P. M. Weaver, K. Potter, Computer aided modelling of variable angle tow composites manufactured by continuous tow shearing, Composite Structures 129 (2015) 256–267.

[34] C. Waldhart, Analysis of tow-placed, variable-stiffness laminates, Ph.D. thesis, Virginia Polytechnic Institute and State University (1996).

[35] B. Kim, K. Hazra, P. Weaver, K. Potter, Limitations of fibre placement techniques for variable angle tow composites and their process-induced defects.

[36] W. Liu, R. Butler, Buckling optimization of variable-angle-tow panels using the infinite-strip method, AIAA journal 51 (6) (2013) 1442–1449.

[37] R. Groh, P. Weaver, Buckling analysis of variable angle tow, variable thickness panels with transverse shear effects, Composite Structures 107 (2014) 482–493.

[38] R. Groh, P. Weaver, Mass optimization of variable angle tow, variable thickness panels with static failure and buckling constraints, 56th AIAA/ASME/ASCE/AHS/ASC Structures, Structural Dynamics and Materials Conference, AIAA SciTech Forum, (2015), AIAA 2015-0452.

[39] Tsai, S. W., Halpin, J. C., and Pagano, N. J., Composite materials workshop, Vol. 30, No. 11, 1968, pp. 223–53, Stamford, CT: Technomic Publishing Co., Inc.

[40] R. M. Jones, Mechanics of composite materials, CRC Press, 2nd Revised edition edition, 1998.

[41] D. Peeters, M. Abdalla, Optimization of ply drop locations in variable-stiffness composites, AIAA Journal 54 (5) (2016) 1760 – 1768.

[42] D. Peeters, Design Optimisation of Practical Variable Stiffness and Thickness Laminates, Ph.D. thesis, Delft University of Technology, Netherland (2017).

[43] P. S. Bulson, The Stability of Flat Plates, Chatto and Windus Ltd, London, 1970.

[44] O. Seresta, M. M. Abdalla, Z. Gürdal, Approximate internal load prediction in composite structures with locally buckled panels, Journal of Aircraft 45 (2) (2008) 513–522.

[45] K. He, S. Hoa, R. Ganesan, The study of tapered laminated composite structures: a review, Composites Science and Technology 60 (14) (2000) 2643–2657.

[46] D. Peeters, M. Abdalla, Optimisation of variable stiffness composites with ply drops (2015) 0450.

[47] J. Ashton, Approximate solutions for unsymmetrically laminated plates, Journal of Composite materials 3 (1) (1969) 189–191.

[48] A. Leissa, J. Whitney, Analysis of a simply supported laminated anisotropic rectangular plate, AIAA journal 8 (1) (1970) 28–33.

[49] E. H. Mansfield, The bending and stretching of plates, Second Edition, Cambridge University Press, 1989.

[50] C. G. Diaconu, P. M. Weaver, Postbuckling of long unsymmetrically laminated composite plates under axial compression, International Journal of Solids and Structures 43 (223) (2006) 6978 – 6997.

[51] J. E. Herencia, P. M. Weaver, M. I. Friswell, Optimization of anisotropic plates that vary in thicknesses and properties, 16th International Conference on Composite Materials, 2007: 1-10.

[52] R. Vescovini, C. Bisagni, Semi-analytical buckling analysis of omega stiffened panels under multi-axial loads, Composite Structures 120 (2015) 285–299.

[53] C. G. Diaconu, P. M. Weaver, Approximate solution and optimum design of compression-loaded, postbuckled laminated composite plates, AIAA Journal 43 (4) (2005) 906 – 914.

[54] M. Pandey, A. Sherbourne, Postbuckling behaviour of optimized rectangular composite laminates, Composite Structures 23 (1) (1993) 27 – 38.

[55] K. Svanberg, A class of globally convergent optimization methods based on conservative convex separable approximations, SIAM journal on optimization 12 (2) (2002) 555–573.

[56] C. Lopes, Z. Gürdal, P. Camanho, Variable-stiffness composite panels: Buckling and first-ply failure improvements over straight-fibre laminates, Computers & Structures 86 (9) (2008) 897–907.

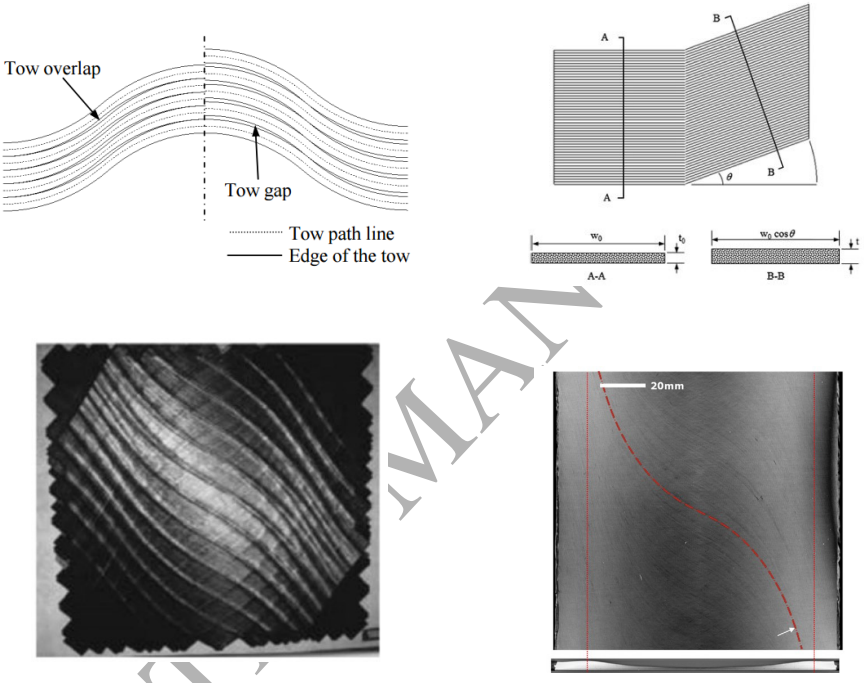

Figure 1: (a) AFP tow-steering illustrative diagram using shifting method and a tow-overlapped VAT Panel [56]; (b) CTS tow shearing procedure and CT-scan images of a CTS-manufactured VAT Panel [32].

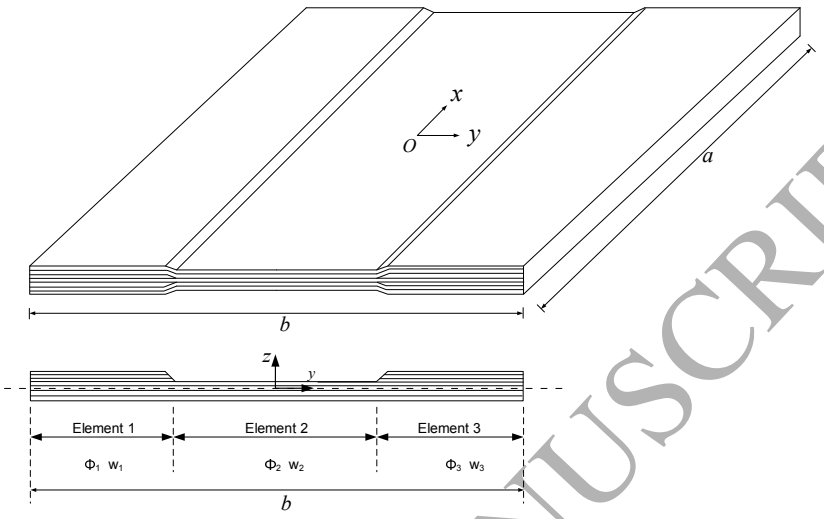

Figure 2: Illustration of a composite plate with discontinuous thickness change and two different cross-sections.

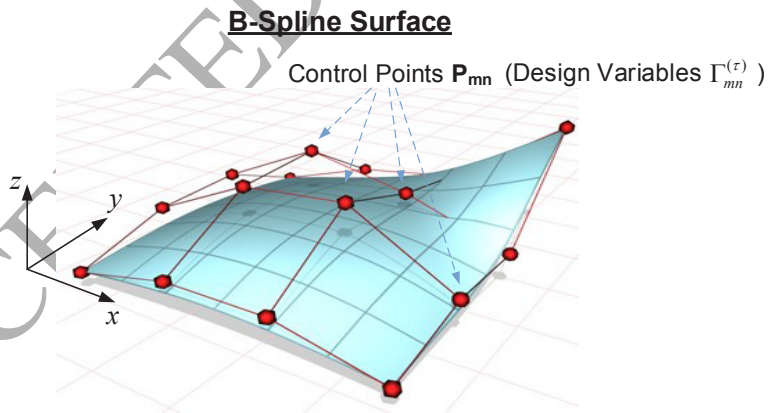

Figure 3: An illustration of B-spline surface constructing by uniformly spaced control points.

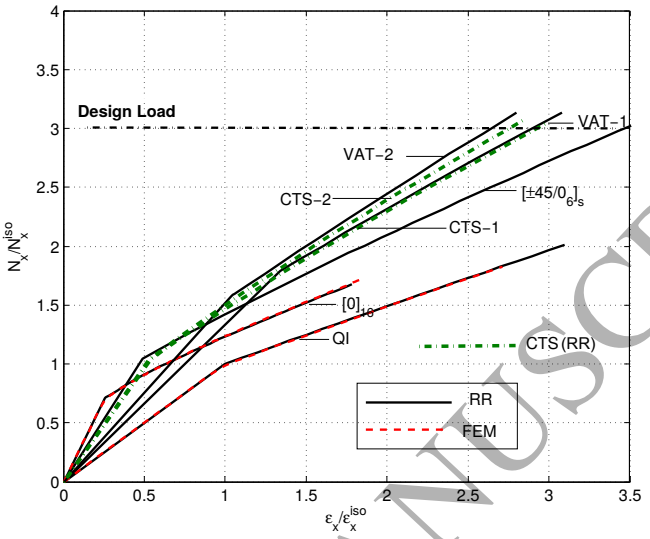

Figure 4: Postbuckling responses of the optimal VAT (constant-thickness) and CTS layups of a square panel under a given uniaxial compressive loading ($N_{x0} = 3N_x^{iso}$) for minimizing the end-shortening strain : Normalized axial loads N_x/N_x^{iso} versus Normalized axial strain $\epsilon_x/\epsilon_x^{iso}$.

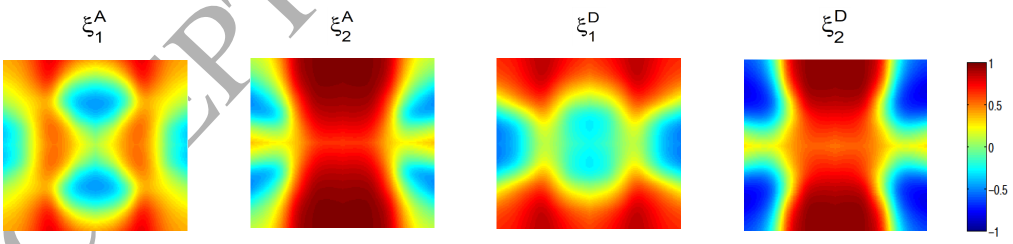

Figure 5: Optimal lamination parameter distribution of a square VAT panel that gives minimum end-shortening strain under a given uni-axial compressive loading ($N_{x0} = 3N_x^{iso}$), 7×7 control points are used in the construction of B-spline surface.

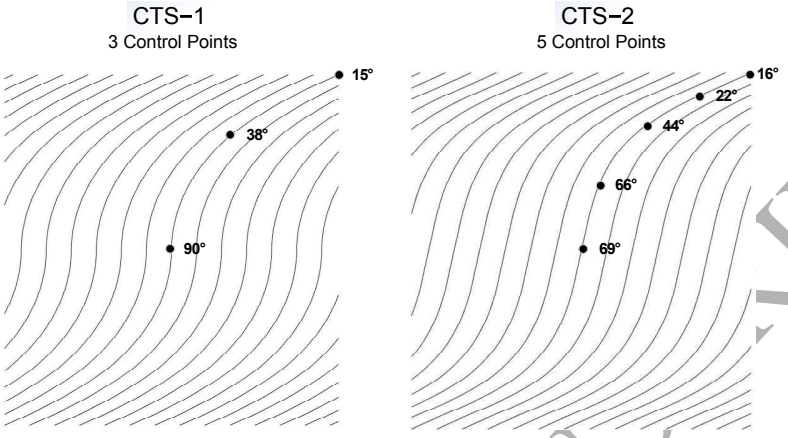

Figure 6: CTS tow trajectories of CTS-1 panel ($[\pm\theta_1(y)/0_4]_s$, defined by 3 control points) and CTS-2 panel ($[\pm\theta_2(y)/0_4]_s$, defined by 5 control points) for the optimal design of postbuckling behaviour as shown in Figure 4.

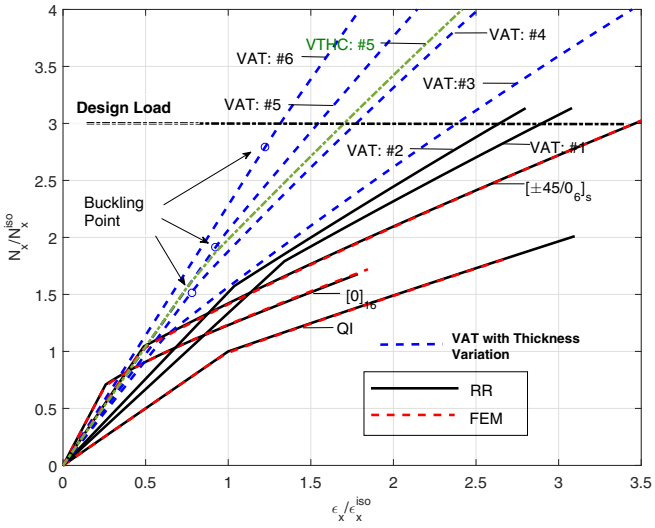

Figure 7: Postbuckling responses of the optimal VAT layups with different thickness variation patterns for a square panel under a given uniaxial compressive loading ($N_{x0} = 3N_x^{iso}$) for minimizing the end-shortening strain: Normalized axial loads N_x/N_x^{iso} versus Normalized axial strain $\epsilon_x/\epsilon_x^{iso}$.

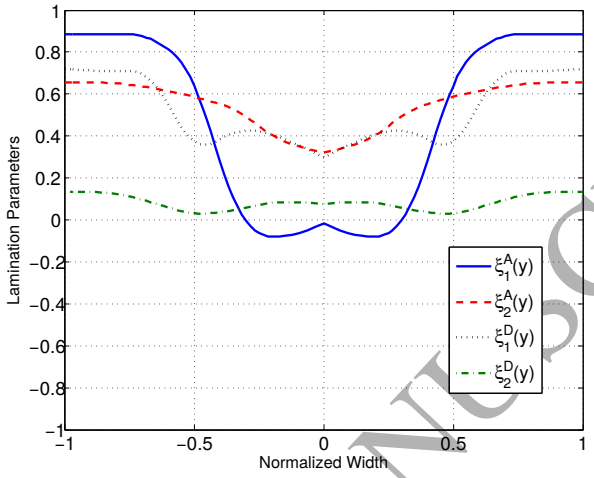

Figure 8: Optimal variations of the four lamination parameters ($\xi_{1,2}^{A,D}$) of VAT panel #5.

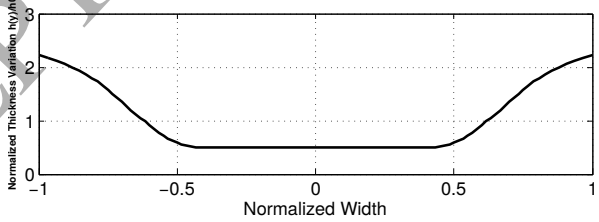

Figure 9: Optimal thickness variation of VAT panel #5 along the loaded edges: Normalized Thickness Variation $h(y)/h_0$ versus Normalized width $\eta = 2y/b$.

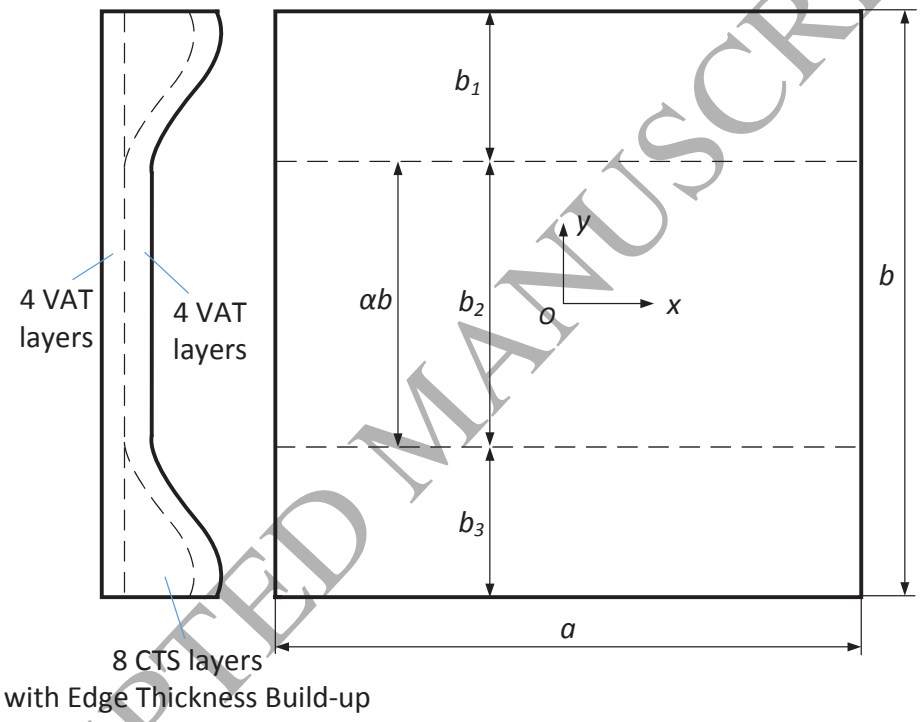

Figure 10: Illustration of a blended VAT panel design with 8 constant thickness VAT plies ($[\pm\theta_1/\pm\theta_1]_s$) over the entire plate and 8 segmentally placed CTS plies at the outer regions ($([\pm\theta_2/\pm\theta_2]_s)$).

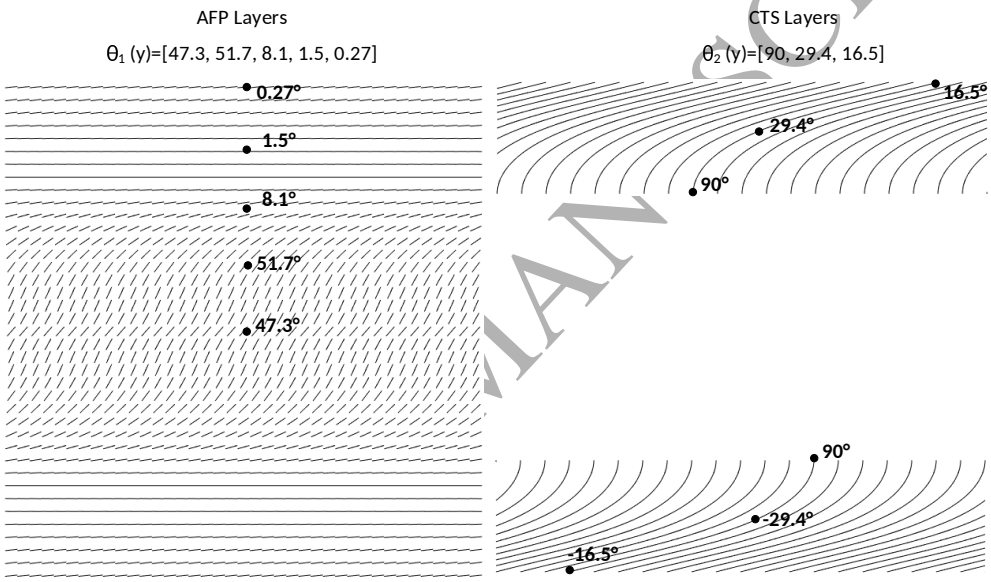

Figure 11: Optimized tow trajectories of constant thickness VAT (AFP-manufactured) plies (θ_1 defined by 5 control points) and CTS plies (θ_2, defined by 3 control points)

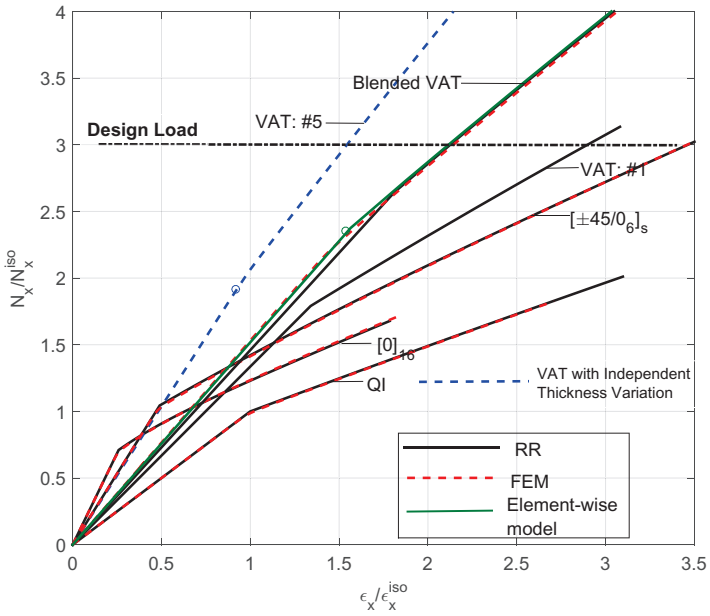

Figure 12: Comparison and validation on the postbuckling response of the optimal blended VAT panel using different modelling methods: FEM, basic postbuckling model in Eq. (5) and the element-wise method in Eq. (22).